Controlling aggregation and crystallization of solution processed diketopyrrolopyrrole based polymer for high performance thin film transistors by pre-metered slot die coating process

Author

Chang, Jingjing, Sonar, Prashant, Lin, Zhenhua, Zhang, Chunfu, Zhang, Jie, Hao, Yue, Wu, Jishan

Published

2016

Journal Title

Organic Electronics

Version

Submitted Manuscript (SM)

DOI

10.1016/j.orgel.2016.06.003

Controlling Aggregation and Crystallization of Solution Processed Diketopyrrolopyrrole Based Polymer for High Performance Thin Film Transistors by Introducing Solvent Additive

*Jingjing Chang, Prashant Sonar, Zhenhua Lin, Jie Zhang,** and *Jishan Wu**

Prof. J. Wu, J. Chang,
Department of Chemistry, National University of Singapore, 3 Science Drive 3, 117543, Singapore, E-mail: chmwuj@nus.edu.sg
Prof. J. Wu, J. Chang, Dr. Z. Lin, Dr. J. Zhang,
Institute of Materials Research and Engineering, A*STAR, 3 Research Link, 117602, Singapore
E-mail:wuj@imre.a-star.edu.sg and zhangj@imre.a-star.edu.sg
Prof. P. Sonar,
School of Chemistry, Physics and Mechanical Engineering, Queensland University of Technology (QUT), 2 George Street, Brisbane, QLD-4001, Australia.
Dr. Z. Lin,
Department of Electrical and Computer Engineering, National University of Singapore, 10 Kent Ridge Crescent, Singapore 119260, Singapore

Abstract

The organic semiconductors have received much attention for plastic electronics due to their good solution processability, low temperature deposition, and compatible with large-area printing technology. The charge transport properties of polymer based field effect transistors are limited by their amorphous domains and weakly interaction between polymer chains. Here, anti-solvent (methanol) is chosen in this study to promote polymer aggregation in solution, and slot die coating was used to fine tune the morphology. The effects of anti-solvent introduction and slot die coating process on the device performance, e.g. charge transport, surface morphology, and solid state packing, were investigated in details. By optimizing the anti-solvent ratio and aggregation degree, the charge transport properties of the polymer devices were observed to significantly improved, average charge carrier mobility of 3.76 $cm^2V^{-1}s^{-1}$ and a maximum mobility of 4.10 $cm^2V^{-1}s^{-1}$ were achieved under optimized conditions. The controlling the aggregation degree by combining the solvent system and slot die coating technique provide a convenient and practical approach to achieve high performance polymer field effect transistors devices.

Introduction

Organic field-effect transistors (OFETs) have attracted great attention within the last few decades due to their potential applications in low cost and flexible electronics.[1–12] Significant progress has been made for polymer-based field effect transistors because of their solution processability, low temperature deposition, and the mechanical robustness for flexible and large area applications.[13–15] Compared to small molecule with high crystallization behavior, the polymer crystallization is weaker, which ensures the film uniformity, but limits the charge transport along the large crystal domains due to the presence of amorphous regions. Recently, the polymeric materials based field effect transistors especially for diketopyrrolopyrrole (DPP)-based π-conjugated copolymers have been reported with charge carrier mobility exceeding 1.0 $cm^2\ V^{-1}s^{-1}$, which are comparable to traditional amorphous silicon based transistors.[16–22] The low-temperature solution processability of these polymeric materials makes them more promising to replace the amorphous silicon in future plastic electronics.

Using solvent additive to control the small molecule crystallization has been reported previously. Taking the 2,7-dioctyl[1]benzothieno[3,2-b][1] benzothiophene (C8-BTBT) small molecule as an example, antisolvent *N*,*N*-dimethylformamide (DMF) was added into the 1,2-dichlorobenzene (DCB) solution to control the semiconductor C8-BTBT single-crystal or polycrystalline thin films growth at the liquid–air interfaces. Using this approach, the author achieved single crystalline thin-film transistors with carrier mobility as high as 16.4 $cm^2V^{-1}\ s^{-1}$ for ink-jet printed devices.[23] For TIPS-pentacene, several groups have reported using mixed solvent systems to enhance the thin film crystallinity, and achieved highly crystalline thin film transistor with charge carrier mobility up to 3.2 $cm^2V^{-1}\ s^{-1}$.[21-22, 24]

Using solvent additives or mixed solvents to enhance the polymer crystallization were also reported in the literatures.[25–27] The utilized solvent additives like 1,8-diiodooctane and 1-chloronaphthalene (CN) were also observed in the formation of bulk heterojunction (BHJ) films from polymer:fullerene blends due to

solution-phase polymer aggregation.[28,29] It was found that proper additives could enhance the film crystallinity and phase separation. For polymer aggregation, it can enhance the thin film crystallinity by forming ordered self-assembled structure.[30] In OFET devices, it was proposed that in high-molecular-weight semiconducting polymers the limiting charge transport step is trapping caused by lattice disorder, and that short-range intermolecular aggregation is sufficient for efficient long-range charge transport.[30] Hence, how to control the polymer chain aggregation becomes the key issue to achieve high-performance polymer thin film transistors.

Recently, several film alignment deposition techniques were developed to enhance the organic semiconductor film crystallinity and morphology,[32–33] such as dip-coting,[34] solution-shearing,[35] and slot die coating[26]. Among these methods, slot die coating has proven to be a simplistic and manufacturable approach to fabricate large area high performance thin film transistors. Most importantly, it was found that this method is not only suitable for small molecule system like TIPS-pentacene,[24] but also useful for polymer systems like PDPPT-TT. This technique saves raw materials and controls film uniformity reliably, accurately, and reproducibly. The slot die coating is scalable to large areas and is, therefore, applicable for the fabrication of large area low cost electronics.

In this study, we reported highly crystalline solution processed DPP based polymer PDPPF-DTT for high performance thin film transistors achieved by adding solvent additive and further controlled by slot die coating. It was found that the proper aggregation of the polymer crystals could enhance the polymer film solid state order and improve the surface morphology. Most importantly, the aggregation degree could be well controlled by the slot die coating speeds, hence change the surface morphologies. Finally, the electrical properties could be changed as well.

Results and discussion

In order to promote proper aggregation to enhance polymer thin film crystallinity, varying amounts of anti-solvent methanol (MeOH) were added to chloroform solutions of PDPPF-DTT. Figure 1 shows the ultraviolet–visible (UV−Vis) spectra of

the thin films without and with MeOH additive. When addition of MeOH to PDPPF-DTT solutions was 1:5 or less by volume, the UV-Vis spectra of the thin films exhibited almost no shift in λ_{max} compared to polymer film processed from pure chloroform solution. However, when the amount of MeOH additive increased to 30%, by volume, the UV-Vis spectra of the resulted thin film exhibited a large red shift which indicates an enhanced polymer aggregation due to strong inter-chain interaction.[36]

To further examing the thin film microstructure change, the two-dimensional X-ray diffraction (2D XRD) was performed. It was found that films produced from these $CHCl_3$/MeOH solutions showed a series of (l00) diffraction peaks and with large increment in diffraction intensities which indicates an improvement in thin film crystallinity. However, the diffraction intensity decreased when further increasing the MeOH additive content to 30%, indicating that larger aggregation content could reduce the thin film crystallinity and quality. The in-plane information was also checked by transmission XRD with X-ray parallel to the thin film stack. As shown in Figure 1d, the 2D XRD pattern clearly showed similar laminar packing mode with out-of-plane diffraction of the spin coated thin films, and the d-spacing value is determined to be 1.83 nm, which is similar to the information obtained from the thin film that was spin coated on OTS modified SiO_2 substrates. In addition, a broad diffraction pattern related to in-plane information was observed which is overlapped by the side-chain packing and π-π stacking peaks.[37] The estimated spacing values were 0.43 nm and 0.37 nm, respectively. The π-π stacking distance is similar to most of DPP based conjugated polymers.[17,38]

To investigate the effect of the solvent additive on surface morphologies, the surface properties were investigated by tapping-mode atomic force microscopy (AFM). The increasing domain size and film roughness were observed when MeOH additive was added to the $CHCl_3$ solution. For example, when increasing the MeOH ratio up to 30% by volume, large aggregates and crystalline nanofibers were observed. As shown in Figure 2, the surface roughness values have almost no change at lower volume ratio of MeOH, and showed smooth surface with RMS of 2.16 nm for control

device, 1.60 nm for 10% volume ratio, and 1.88 nm for 20% volume ratio, respectively. However, with a high ratio (30%) of MeOH additive, the surface roughness significantly increased to 17.4 nm, indicating a higher degree film aggregation. The surface features were further characterized by the HR-TEM measurement, as shown in Figure S2, and the increased domain size could be observed.

To investigate the effect of MeOH additives on the electrical properties of these PDPPF-DTT films, the filed effect transistors were built with PDPPF-DTT films processed from solutions with different volume percentage of MeOH. As shown in Figure 3, the transfer curves revealed a slightly increased field-effect mobility, up to a maximum hole mobility of 2.8 $cm^2/V^{-1}s^{-1}$ when the solution contains 20% MeOH additive compared to pure solvent processed device (2.6 $cm^2/V^{-1}s^{-1}$). Further increasing the MeOH additive to 30% in volume, the charge carrier mobility significantly decreased to 0.13 $cm^2V^{-1}s^{-1}$ due to the deterioration of the thin film formations. This additive-induced aggregation promoted the thin films crystallinity, but less improvement in charge carrier mobility. These results suggest that the PDPPF-DTT crystal domains were random orientated rather than that of in-plane along π-stacking orientations and the aggregation induced defects existed in the thin films, therefore, the transistor device performance were less improved.

To improve the high crystalline thin film's morphology, the external shearing force was introduced by using slot-die coating technique.[24] This well-developed technique -slot die coating has a good control on the film self-assembly and alignment of these large crystal domains of the polymer thin film processed from the mixed solvent systems. The scheme of the process is shown in Figure 4. The working mechanism is simple with the substrates being fixed by a temperature-controlled vacuum suction plate and preheated to required temperature. A small volume of polymer solution was coated on the substrate surface by a slot die with different coating speeds ranging from 0.1 – 1.5 mm/s. The pre-exposed seeding film can act as the nucleation site for remaining molecules in the solution to grow along the coating direction. The solution with 20% MeOH additive was used due to its enhanced

crystallinity. At the different coating speeds, we demonstrated the controlled polymer aggregation in the thin film. At lower coating speed, the time for solvent evaporation is long, which extended the time for polymer aggregation and grown in the size due to decreased polymer solubility, while at the higher coating speed, the aggregation is less due to the fast drying film with limited time for polymer aggregation. With process optimization, the thin films processed from the polymer solution formed well aligned nanofibers onto the substrates, see Figure 5.

To study the slot die coating effect on the surface morphology and microstructure, the UV-Vis spectroscopy and 2-D XRD were performed on the thin films at different coating speed. The results are shown in Figure 4. The thin film absorption maxima exhibited a red shift with increasing the aggregation degree induced by lower coating speed. The absorption maxima increased from 768 nm (1.5 mm/s) to 771 nm (1.0 mm/s), 775 nm (0.7 mm/s), 781 nm (0.5 mm/s), 800 nm (0.3 mm/s), and 837 nm (0.1 mm/s). with the closely monitoring the degree of polymer aggregation with slot die coating speed, the polymer thin film formation can be fine-tuned for controlled semiconductor properties. The thin film XRD spectra were shown in Figure 4d. The diffraction intensity increased upon increasing the coating speeds due to increased film quality and crystallinity.

The surface morphology of the aligned thin film is shown in Figure 5. At lower coating speed, many large aggregates are observed, and these aggregates could be reduced by increasing the coating speed. This is consistent with the UV-Vis spectra observed. At optimized coating speed (1.0-1.5 mm/s), the smooth and crystalline polymer thin films could be achieved which should be beneficial to the charge carrier transport due to decreased surface defect by these aggregates.

The electrical properties of these controlled thin films were investigated by the OFET devices which were fabricated using the slot die coated PDPPF-DTT film as organic semiconductor. Figure 6 exhibited typical transfer characteristics of spin coated and slot die coated devices. All the devices showed ambipolar behavior with p-type dominated transport when being measured in N_2-filled glovebox. The device parameters such as charge carrier mobilities, current on/off ratio, and threshold

voltage were summarized in Table S1. The average mobilities of the OFETs were obtained from 32 devices for each process condition. As shown in Figure 6, the thin film direct processed from spin coating exhibited charge carrier mobility of 1.1 $cm^2V^{-1}s^{-1}$, and on/off ratio of 10^2-10^3. When using slot die coating, the external shearing force induced by slot die smoothed and ordered the thin films, which resulted increased charge carrier mobility ranging from 1.3 $cm^2V^{-1}s^{-1}$ to 3.7 $cm^2V^{-1}s^{-1}$ at different coating speeds. At the optimized coating speed (0.7 mm/s), the OFET device exhibited the maximum charge carrier mobility of 3.76 $cm^2V^{-1}s^{-1}$, which is 3 times higher than the mobility obtained from the spin coated devices. The mobility as a function of coating speed was shown in Figure 6b. The enhancement of the device performance can be attributed to the increased thin film quality and decreased surface defects due to the controlled aggregation behaviors. The performances of the OFET devices showed temperature dependency, which could be used as thermal sensors. As shown in Figure 6c, the OFET devices showed good temperature response from room temperature to 60 ^oC with a step of 5 ^oC. The linear relationship between source-drain current and temperature could be deduced from Figure 6d. This behavior could be explained by the charge hopping mechanism, which is governed by the Arrhenius law.[39,40]

Conclusions

In summary, high performance slot die coated polymer thin film transistor was processed through inducing MeOH additive into the semiconductor solution have been demonstrated. The surface morphologies, molecular packing, and electrical properties of the polymer devices were investigated in details. It was found that proper MeOH additive could induce a higher degree of aggregation with controlled orientation using slot die coating. Thus, the molecular packing and film crystallinity were both improved. For the polymer thin film prepared from slot die coating approach, the OFET using the highly crystalline thin films as semiconductor showed enhanced charge carrier mobility as high as 3.76 $cm^2V^{-1}s^{-1}$.

Experimental Section

Materials: The copolymer PDPPF-DTT was synthesized according to the procedure which will be published elesewhere.[41]

OFET fabrication: Top-contact devices were prepared in ambient air. A heavily *n*-doped silicon wafer with a 200-nm thermal SiO_2 layer was used as the substrate/gate electrode. The SiO_2/Si substrate was cleaned with acetone, isopropyl alcohol (IPA), and then immersed in a piranha solution (H_2SO_4: H_2O_2 = 2:1) for 8 minutes, followed by rinsing with deionized water. The OTS treatments were done by vapor treatment for 3h at 120 ^oC in the vacuum. The semiconductor layer was deposited on top of the organosilanes modified SiO_2 by coating the semiconductor solution PDPPF-DTT in chloroform solvent with a concentration of 6 mg/mL without and with MeOH additive) with spin coater or slot die coater (Coatmaster Model 510). The thin films were then annealed at 240 ^oC for 10 min. Subsequently, gold source/drain electrodes were deposited by thermal evaporation through a metal shadow mask to complete the OFETs with various channel length (L = 50 - 100 um) and width (W = 1 mm). The OFET devices were then characterized using a Keithley SCS-4200 probe station in ambient air or in N_2 glovebox (dark). The temperature measurement was controlled by the temperature controller from Scientific Instrument (model 9700). To minimize the leakage current, small trenches in the thin film around the electrodes were created with a needle. The devices were isolated to reduce the fringing effects which can induce an overestimation of drain current and large leakage current.

Surface morphology and microstructure characterization: AFM images were recorded on a tapping mode atomic force microscopy (AFM) (Bruker ICON-PKG AFM). XRD measurements were performed on a 2D GADDS X-ray diffraction (Bruker-AXS D8 DISCOVER GADDS). UV-Vis absorption spectra were recorded on a Shimadzu UV-1800 spectrophotometer.

Supporting Information

Supporting Information is available from the Wiley Online Library or from the author.

Acknowledgements

This work was financially supported by MOE Tier 2 grant (MOE2014-T2-1-080), Tier 3 Programme (MOE2014-T3-1-004), A*STAR-DST Joint Grant (IMRE/14-2C0239), and SERC Printed Electronics Program (Grant #1021700134 and #1021700137).

Reference

[1] S. Park, G. Wang, B. Cho, Y. Kim, S. Song, Y. Ji, M.-H. Yoon, T. Lee, *Nat. Nanotechnol.* **2012**, *7*, 438.

[2] D. Tobjörk, R. Österbacka, *Adv. Mater.* **2011**, *23*, 1935.

[3] H. Yan, Z. Chen, Y. Zheng, C. Newman, J. R. Quinn, F. Dötz, M. Kastler, A. Facchetti, *Nature* **2009**, *457*, 679.

[4] S. Allard, M. Forster, B. Souharce, H. Thiem, U. Scherf, *Angew. Chem. Int. Ed.* **2008**, *47*, 4070.

[5] M. Mas-Torrent, C. Rovira, *Chem. Soc. Rev.* **2008**, *37*, 827.

[6] Y. Yang, F. Wudl, *Adv. Mater.* **2009**, *21*, 1401.

[7] J. Li, J.-J. Chang, H. S. Tan, H. Jiang, X. Chen, Z. Chen, J. Zhang, J. Wu, *Chem. Sci.* **2012**, *3*, 846.

[8] J. Sun, B. Zhang, H. E. Katz, *Adv. Funct. Mater.* **2011**, *21*, 29.

[9] J. Chang, H. Qu, Z.-E. Ooi, J. Zhang, Z. Chen, J. Wu, C. Chi, *J. Mater. Chem. C* **2013**, *1*, 456.

[10] Y. Wen, Y. Liu, *Adv. Mater.* **2010**, *22*, 1331.

[11] K. Fukuda, Y. Takeda, Y. Yoshimura, R. Shiwaku, L. T. Tran, T. Sekine, M. Mizukami, D. Kumaki, S. Tokito, *Nat. Commun.* **2014**, *5*, 4147.

[12] J. Chang, J. Shao, J. Zhang, J. Wu, C. Chi, *RSC Adv.* **2013**, *3*, 6775.

[13] M. Uno, K. Nakayama, J. Soeda, Y. Hirose, K. Miwa, T. Uemura, A. Nakao, K. Takimiya, J. Takeya, *Adv. Mater.* **2011**, *23*, 3047.

[14] G. H. Gelinck, H. E. a Huitema, E. van Veenendaal, E. Cantatore, L. Schrijnemakers, J. B. P. H. van der Putten, T. C. T. Geuns, M. Beenhakkers, J. B. Giesbers, B.-H. Huisman, E. J. Meijer, E. M. Benito, F. J. Touwslager, A. W. Marsman, B. J. E. van Rens, D. M. de Leeuw, *Nat. Mater.* **2004**, *3*, 106.

[15] G. Dai, J. Chang, J. Wu, C. Chi, *J. Mater. Chem.* **2012**, *22*, 21201.

[16] C. B. Nielsen, M. Turbiez, I. McCulloch, *Adv. Mater.* **2013**, *25*, 1859.

[17] Y. Li, S. P. Singh, P. Sonar, *Adv. Mater.* **2010**, *22*, 4862.

[18] Z. Chen, M. J. Lee, R. Shahid Ashraf, Y. Gu, S. Albert-Seifried, M. Meedom Nielsen, B. Schroeder, T. D. Anthopoulos, M. Heeney, I. McCulloch, H. Sirringhaus, *Adv. Mater.* **2012**, *24*, 647.

[19] J. Li, Y. Zhao, H. S. Tan, Y. Guo, C.-A. Di, G. Yu, Y. Liu, M. Lin, S. H. Lim, Y. Zhou, H. Su, B. S. Ong, *Sci. Rep.* **2012**, *2*, 754.

[20] H. Bronstein, Z. Chen, R. S. Ashraf, W. Zhang, J. Du, J. R. Durrant, P. S. Tuladhar, K. Song, S. E. Watkins, Y. Geerts, M. M. Wienk, R. A. J. Janssen, T. Anthopoulos, H. Sirringhaus, M. Heeney, I. Mcculloch, *J. Am. Chem. Soc.* **2011**, *133*, 3272.

[21] Y. Li, P. Sonar, L. Murphy, W. Hong, *Energy Environ. Sci.* **2013**, *6*, 1684.

[22] I. Kang, T. K. An, J. Hong, H.-J. Yun, R. Kim, D. S. Chung, C. E. Park, Y.-H. Kim, S.-K. Kwon, *Adv. Mater.* **2013**, *25*, 524.

[23] H. Minemawari, T. Yamada, H. Matsui, J. Tsutsumi, S. Haas, R. Chiba, R. Kumai, T. Hasegawa, *Nature* **2011**, *475*, 364.

[24] J. Chang, C. Chi, J. Zhang, J. Wu, *Adv. Mater.* **2013**, *25*, 6442.

[25] J. A. Lim, J.-H. Kim, L. Qiu, W. H. Lee, H. S. Lee, D. Kwak, K. Cho, *Adv. Funct. Mater.* **2010**, *20*, 3292.

[26] B.-G. Kim, E. J. Jeong, J. W. Chung, S. Seo, B. Koo, J. Kim, *Nat. Mater.* **2013**, *12*, 659.

[27] T. K. An, I. Kang, H. J. Yun, H. Cha, J. Hwang, S. Park, J. Kim, Y. J. Kim, D. S. Chung, S. K. Kwon, Y. H. Kim, C. E. Park, *Adv. Mater.* **2013**, *25*, 7003.

[28] J. K. Lee, W. L. Ma, C. J. Brabec, J. Yuen, J. S. Moon, J. Y. Kim, K. Lee, G. C. Bazan, A. J. Heeger, *J. Am. Chem. Soc*. **2008**, *130*, 3619.

[29] A. K. K. Kyaw, D. H. Wang, C. Luo, Y. Cao, T.-Q. Nguyen, G. C. Bazan, A. J. Heeger, *Adv. Energy Mater.* **2014**, *4*, 1301469.

[30] S. Kim, T. K. An, J. Chen, I. Kang, S. H. Kang, D. S. Chung, C. E. Park, Y.-H. Kim, S.-K. Kwon, *Adv. Funct. Mater.* **2011**, *21*, 1616.

[31] R. Noriega, J. Rivnay, K. Vandewal, F. P. V Koch, N. Stingelin, P. Smith, M. F. Toney, A. Salleo, *Nat. Mater.* **2013**, *12*, 1038.

[32] M. O'Neill, S. M. Kelly, *Adv. Mater.* **2011**, *23*, 566.

[33] S. Liu, W. M. Wang, A. L. Briseno, S. C. B. Mannsfeld, Z. Bao, *Adv. Mater.* **2009**, *21*, 1217.

[34] H. N. Tsao, D. Cho, J. W. Andreasen, A. Rouhanipour, D. W. Breiby, W. Pisula, K. Müllen, *Adv. Mater.* **2009**, *21*, 209.

[35] J. Shin, T. R. Hong, T. W. Lee, A. Kim, Y. H. Kim, M. J. Cho, D. H. Choi, *Adv. Mater.* **2014**, *26*, 6031.

[36] R. Steyrleuthner, M. Schubert, I. Howard, B. Klaumünzer, K. Schilling, Z. Chen, P. Saalfrank, F. Laquai, A. Facchetti, D. Neher, *J. Am. Chem. Soc.* **2012**, *134*, 18303.

[37] I. McCulloch, M. Heeney, M. L. Chabinyc, D. DeLongchamp, R. J. Kline, M. Cölle, W. Duffy, D. Fischer, D. Gundlach, B. Hamadani, R. Hamilton, L. Richter, A. Salleo, M. Shkunov, D. Sparrowe, S. Tierney, W. Zhang, *Adv. Mater.* **2009**, *21*, 1091.

[38] P. Sonar, S. P. Singh, Y. Li, M. S. Soh, A. Dodabalapur, *Adv. Mater.* **2010**, *22*, 5409.

[39] V. Coropceanu, J. Cornil, D. A. da Silva Filho, Y. Olivier, R. Silbey, J-L. Bredas, *Chem. Rev.* **2007**, *107*, 926.

[40] M. Barra, F. V. Di Girolamo, F. Chiarella, M. Salluzzo, Z. Chen, a. Facchetti, L. Anderson, a. Cassinese, *J. Phys. Chem. C* **2010**, *114*, 20387.

[41] P. Sonar, J. Chang, Z. Shi, J. Li, submitted to Materials Horizons.

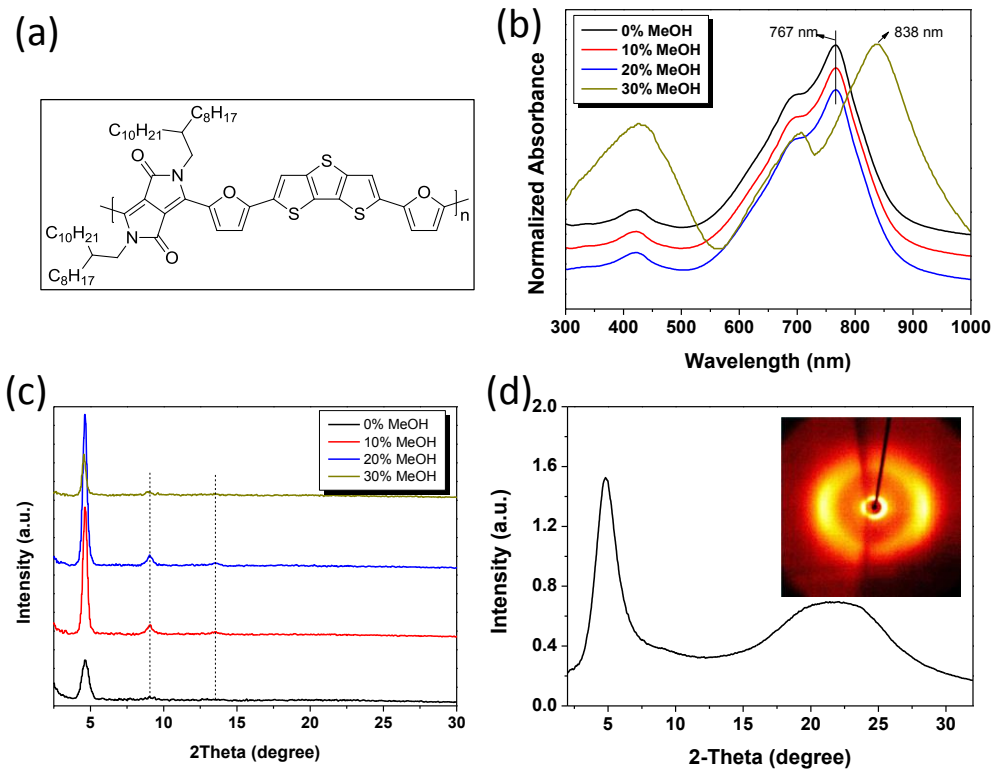

Figure 1. (a) The molecular structure of PDPPF-DTT; (b) UV-Vis absorption spectra of PDPPF-DTT thin films with different contents of MeOH additive; (c) XRD pattern of spin coated thin films on OTS treated substrates with different contents of MeOH additive; (d) 2D transmission XRD spectra with incident X-ray parallel to the thin film stack (inset is the corresponding diffraction image).

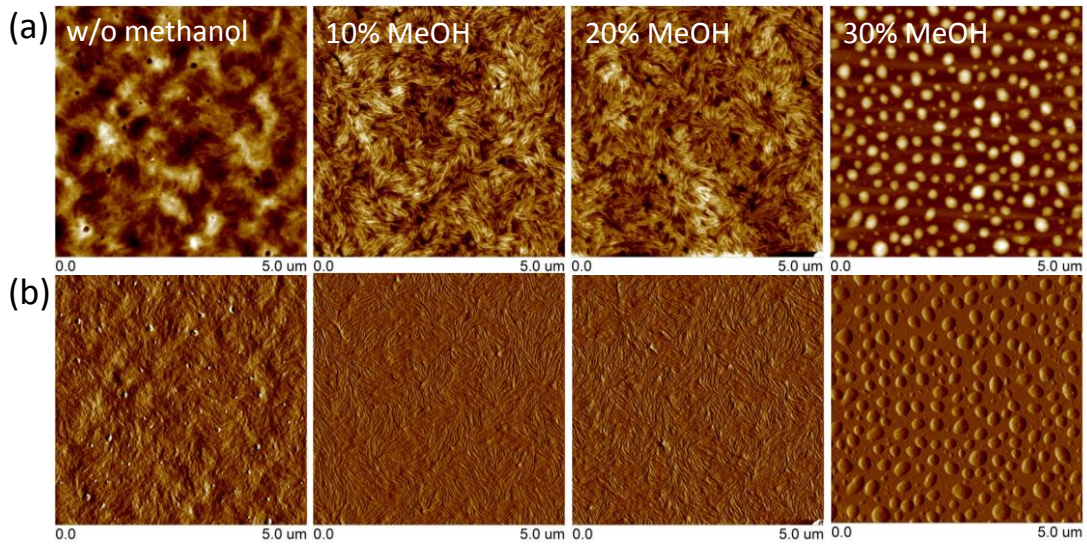

Figure 2. AFM height (a) and phase (b) images of spin coated thin films on OTS treated substrates with different contents of MeOH additive.

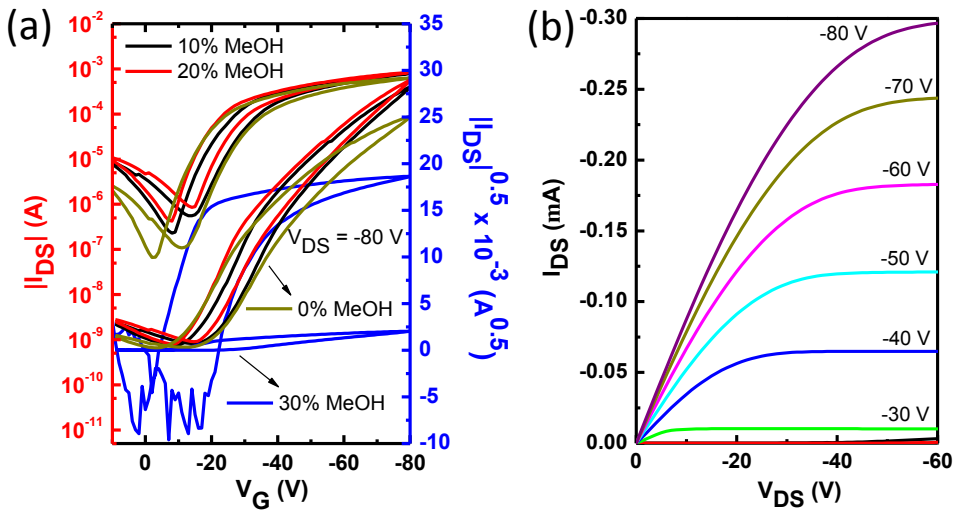

Figure 3. (a) The transfer characteristics of the thin film devices processed with different contents MeOH additives; (b) The output characteristics of the thin film device based on 20% MeOH additive.

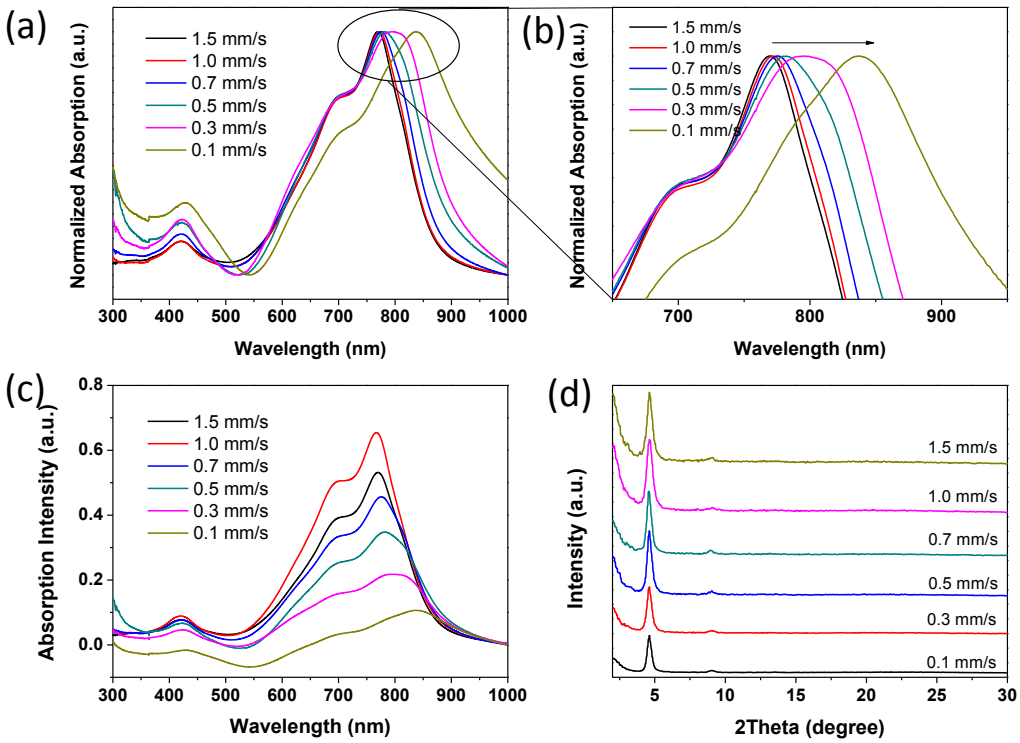

Figure 4. (a) Normalized UV-Vis absorption spectra and corresponding zoom-in image (b) of PDPPF-DTT thin films processed from different coating speed conditions; (c) the UV-Vis spectra of various thin films processed from different coating speed conditions without normalized condition; (d) the XRD spectra of the thin films processed from different coating speed conditions normalized with the thickness.

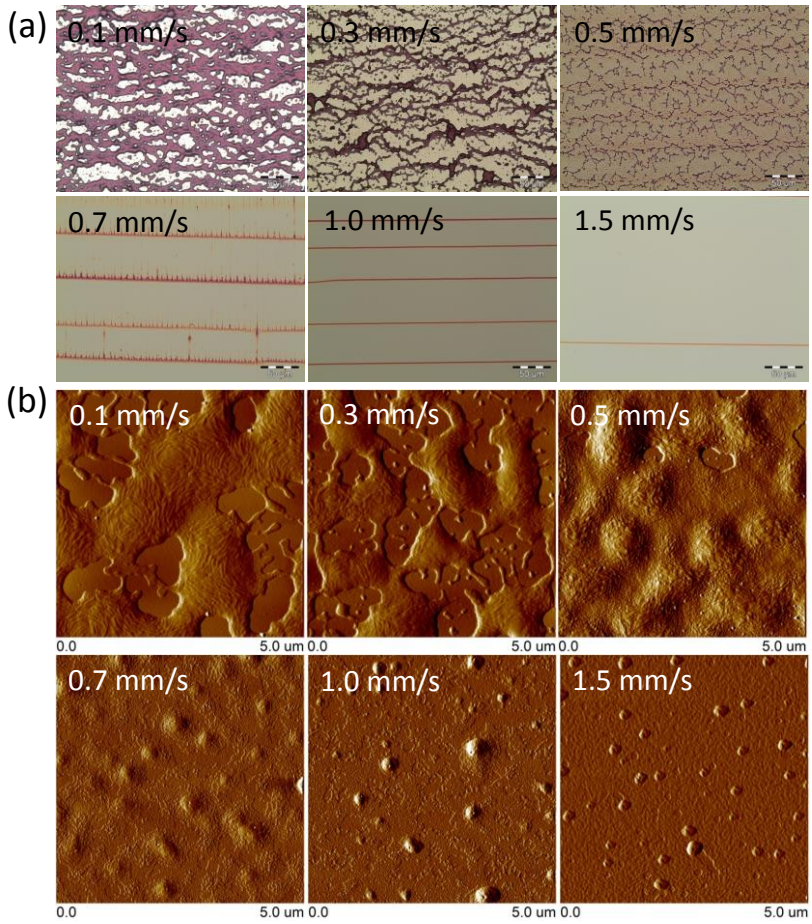

Figure 5. Optical microscopy images (a) and corresponding AFM images (b) of various thin films with different coating speed conditions from 0.1 mm/s to 1.5 mm/s.

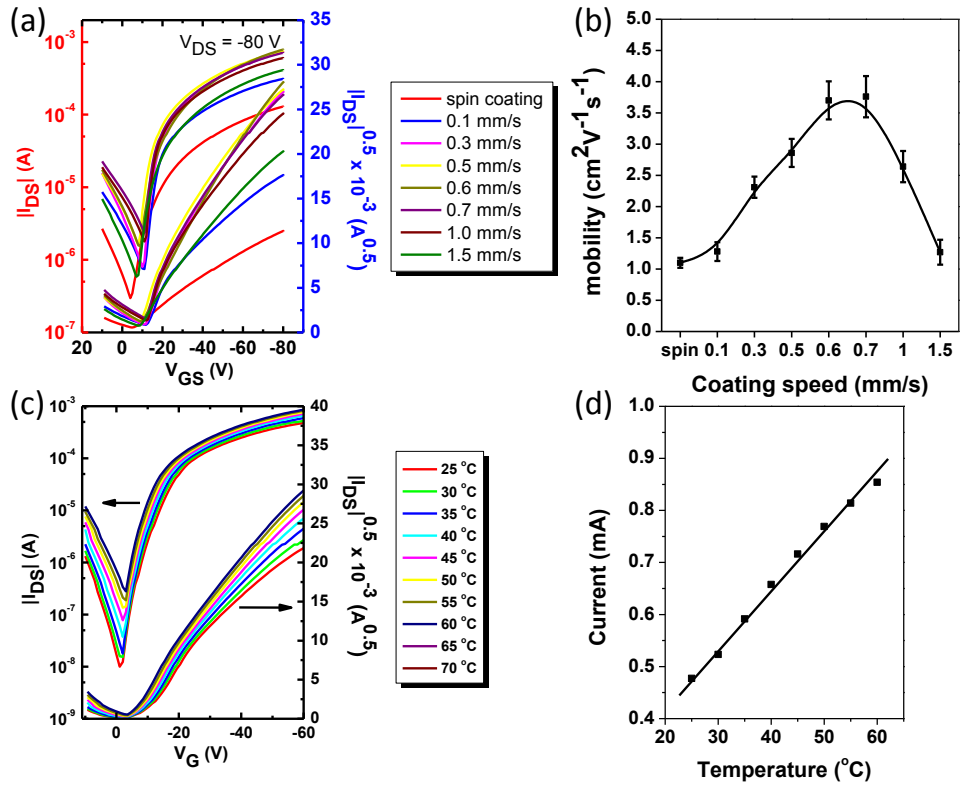

Figure 6. (a) transfer curves of the PDPPF-DTT thin film devices processed with different coating speeds from 0.1 mm/s to 1.5 mm/s; (b) the charge carrier mobility as a function of coating speeds; (c) the transfer characteristics of the thin film device measured under different substrate temperatures; (d) the source-drain current as a function of measurement temperatures.

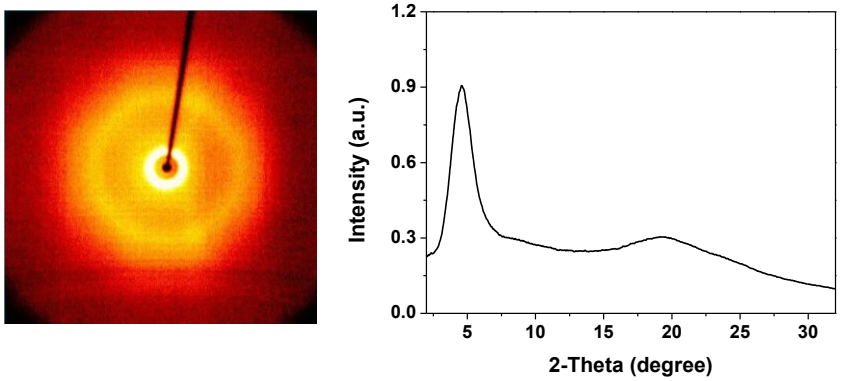

Figure S1. 2D-transmission XRD image and spectra with the X-ray perpendicular to the thin film stack.

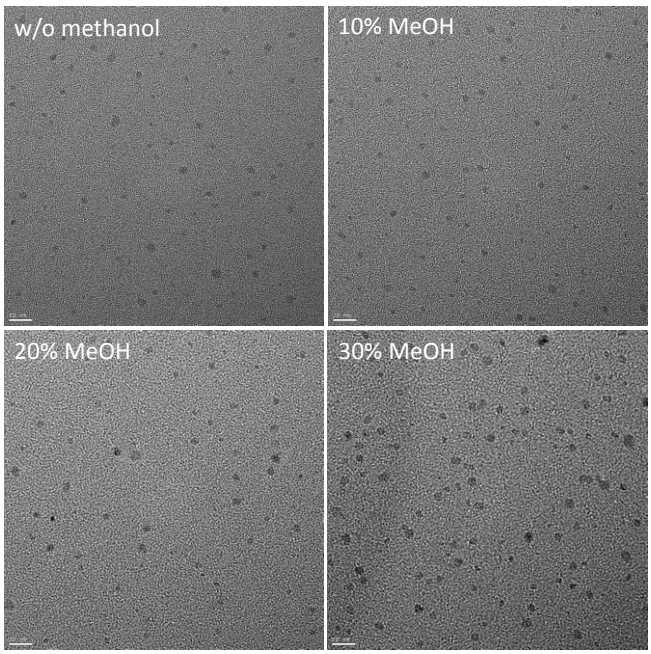

Figure S2. HR-TEM images of the PDPPF-DTT thin film processed from $CHCl_3$/MeOH mixed solvent.

Table S1. The electrical parameters of the thin film devices under different coating speeds.

Polymer	condition	hole		
		$\mu[cm^2V^{-1}s^{-1}]$	V_T [V]	On/off
PDPPF-DTT	Spin coating	1.10±0.08	-10	3.5×10^3
	0.1 mm/s	1.28±0.15	-7	2.4×10^3
	0.3 mm/s	2.31±0.17	-6	5.4×10^3
	0.5 mm/s	2.86±0.23	-6	2.5×10^3
	0.6 mm/s	3.70±0.30	-9	3.4×10^3
	0.7 mm/s	3.76±0.33	-9	4.2×10^3
	1.0 mm/s	2.64±0.25	-8	3.6×10^3
	1.5 mm/s	1.27±0.20	-8	3.8×10^3

TOC

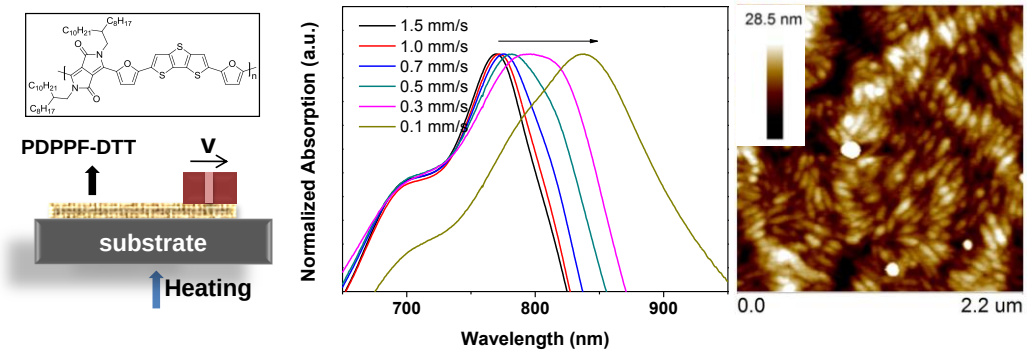

Here, anti-solvent (methanol) is chosen in this study to promote polymer aggregation in solution, and slot die coating was used to fine tune the morphology. High performance OFETs using conjugated copolymer (PDPPF-DTT) as the semiconductor were developed. By optimizing the anti-solvent ratio and aggregation degree, the charge transport properties of the polymer devices were observed to significantly improved, average charge carrier mobility of 3.76 $cm^2V^{-1}s^{-1}$ and a maximum mobility of 4.10 $cm^2V^{-1}s^{-1}$ has been achieved.